DDT Vol. 9, No. 2 January 2004

Atomic force microscopy and drug discovery

J. Michael Edwardson and Robert M. Henderson

Atomic force microscopy is being used ever more widely in biological imaging, because of its unique ability to provide structural information at the single molecule level and under near-physiological conditions. Detailed topographic images of potential drug targets, such as proteins and DNA, have been produced, and the folding of modular proteins has been studied using single-molecule force spectroscopy. Recently, atomic force microscopy has been used to examine ligand–protein and ligand–DNA interactions, and to begin to determine the architecture of multi-subunit proteins, including a member of the superfamily of ionotropic receptors. Atomic force microscopy is fast becoming a valuable addition to the pharmaceutical industry's toolkit.

J. Michael Edwardson
Robert M. Henderson*
Department of Pharmacology
University of Cambridge
Tennis Court Road
Cambridge
UK CB2 1PD
*e-mail: rmh1003@cam.ac.uk

▼ The atomic force microscope was introduced in the late 1980s by Binnig, Quate and Gerber [1], with the intention of producing an instrument that was capable of measuring minute forces 'acting on particles as small as single atoms'. As they hoped, the development of atomic force microscopy (AFM) over the past 17 years has yielded sub-nanometre resolution images together with data on the interactive forces between molecules. In essence, the first microscope of this kind (described in [1]) was a combination of two earlier instruments, the scanning tunnelling microscope [2] and the stylus profilometer [3]. The resulting atomic force microscope works by scanning a fine pyramidal tip back and forth over a surface in a raster pattern. The tip is situated at the end of a micro-engineered cantilever (Figure 1a) and, as it is deflected (repelled by or attracted to the surface), so too is the cantilever. The magnitude of the deflection is registered by the change in direction of a laser beam that is reflected off the end of the cantilever and detected by an array of photomultipliers. Thus, a topological or force map of the surface can be constructed. One of the great advantages of the atomic force microscope, particularly with respect to the imaging of biological specimens, is that it can work in fluid, so that experiments can be performed under near-physiological conditions.

The atomic force microscope

The atomic force microscope can be operated with the tip either touching the sample (contact mode) or oscillating rapidly above the sample (tapping mode). The tapping mode, which works in both air and fluid, produces less lateral force on the substrate [4], a useful feature when investigating relatively delicate and loosely attached biological specimens. The applied vertical force can be minimized by adjustment of the microscope, using a 'force curve' (Figure 1b), at the start of an experiment. To construct the force curve, the cantilever is held stationary (in the horizontal plane) on the substrate, and the tip is lowered towards the surface. As the tip and substrate make contact (during the downward 'approaching' phase of the probe), the cantilever is deflected, and this deflection is registered by the photomultipliers. The tip is then raised and the probe and substrate are drawn apart (during the 'withdrawal' phase). The cantilever is, again, deflected, returning to its original position, but is often further deflected as a result of the attraction of the tip towards the substrate by adhesion forces (which might be chemical or electrostatic). By adjustment of the force curve, these adhesion forces can be minimized. The force curve also provides a measure of the degree of attraction between probe and substrate, and can be used to distinguish different areas of the same sample that have differing physical characteristics and, thus, provide different degrees of attraction to the tip. As a further refinement, force curves can be used in conjunction with specially functionalized tips, to measure the force of

 PII: S1359-6446(03)02905-2

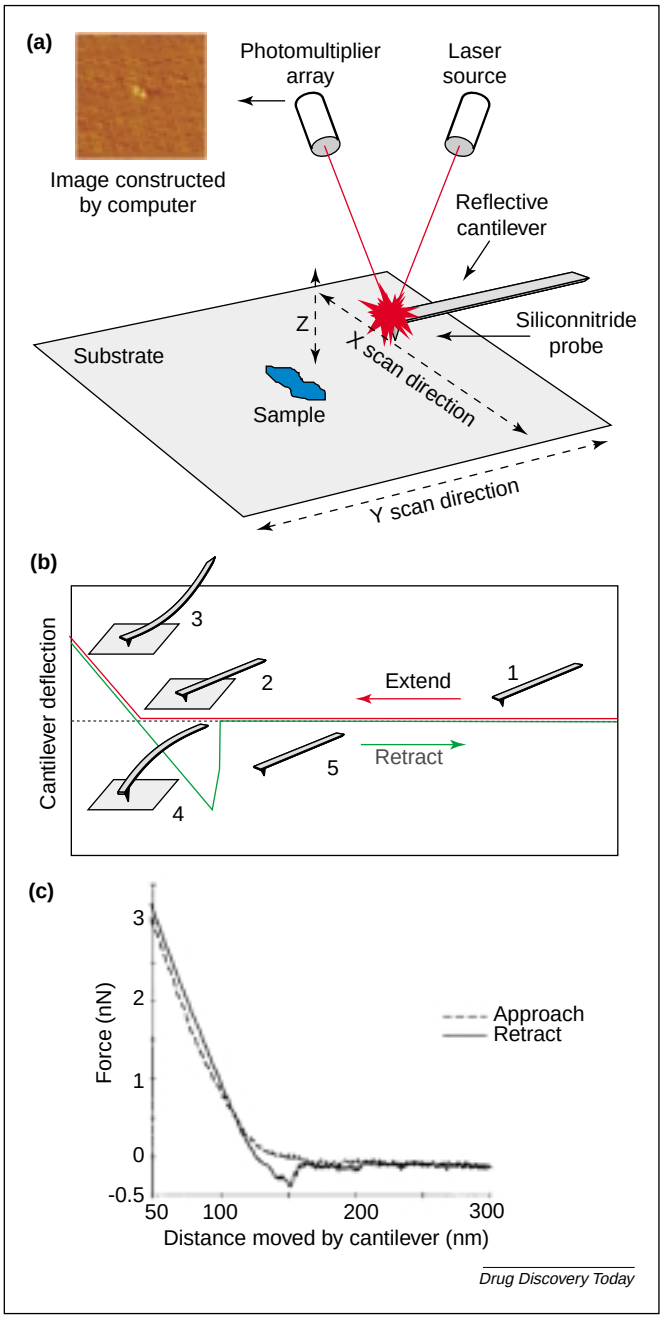

Figure 1. Operation of the atomic force microscope. **(a)** The principle of AFM. A fine pyramidal silicon nitride tip at the end of a reflective cantilever is scanned back and forth over the substrate in a raster pattern. As the tip is deflected by the sample, the cantilever also deflects, and the magnitude of the deflection is registered by the change in direction of a laser beam that is reflected off the end of the cantilever and detected by a photomultiplier array. In this way, a topological map of the surface is constructed. **(b)** The principle of the force curve. The tip is held stationary over the substrate and then oscillated up and down ('extended' and 'retracted'). At point '1' the tip is not in contact with any substrate and so no deflection is registered. At '2' the probe meets the substrate, and at '3′ it is advanced further downwards onto the substrate and so the cantilever bearing the probe is deflected. This is shown in the 'y' axis of the curve. The piezo drivers then begin to withdraw the probe upwards ('retract'). Because the probe and substrate are physically attracted, they maintain contact '4', even when the probe has been withdrawn before the point where it originally made contact with the substrate. At point '5′, the probe loses contact with the substrate and jumps back to its original position, as does the 'retract' curve. The measure of the force of attraction between tip and substrate is given broadly by the size and shape of the triangle lying below the dotted line in the diagram. **(c)** The measurement of the force between a biotinylated AFM tip and a streptavidin-coated substrate. The 'retract' trace shows the breakage of the attachment between streptavidin and biotin and the force measured is approximately 300 pN. Part **(c)** of this figure is adapted from Reference [5].

interaction between biological molecules, such as ligand–receptor pairs. For example, the tip can be coated with biotin, and force curves can be used to study the interaction between biotin and streptavidin (Figure 1c; [5]).

AFM is also being applied, increasingly, to the study of protein unfolding and the nature of intra-molecular interactions within those proteins, using a technique that has become known as 'single-molecule force spectroscopy' [6]. The technique involves attaching the AFM tip to the protein of interest and manipulating the vertical force that is exerted on the molecule by the cantilever. This approach has been applied to proteins of modular construction, such as titin, the molecule that is responsible for the passive elasticity of muscle [7–9], and fibronectin, an important component of the extracellular matrix [10]. The force–extension relationships that are produced have a characteristic 'sawtooth' pattern, caused by the sequential unfolding of the modules within the proteins. Analysis of these data has yielded much information about the molecular mechanisms that are responsible for the mechanical stability of the proteins. Force spectroscopy has also been used to detect conformational changes in single polysaccharide molecules [11,12]. Importantly, these single-molecule measurements have revealed features, such as intermediate and misfolded states, that cannot be observed by using more conventional bulk measurement techniques, such as X-ray crystallography or NMR.

Finally, the atomic force microscope can be used as a 'nano-scalpel' [13]. Macromolecules can be directly manipulated and altered by judicious application of force through the microscope tip. This technique is particularly useful in studying proteins that exist as oligomeric structures; here, nano-dissection can be applied to break down the oligomers, and AFM imaging can reveal structural information about their constituents. For example, AFM has been used to separate gap junctions [14,15]. Müller *et al.* identified conformational changes in the nano-dissected gap junctions when Ca^{2+} was added to the bathing solution, revealing an apparent dependence of gap-junction integrity on the presence of Ca^{2+} [15]. This technique has also been applied with other membrane

proteins, for example, the bacterial porin OmpF [16] and the eye lens water channel, MIP [17].

AFM imaging of pharmaceutical products

From the outset, AFM has lent itself to applications within the pharmaceutical industry. Its value in the examination of structures that might be useful in drug-delivery systems was quickly grasped [18–23]. Recent examples include the investigation of the structure of biodegradable polyanhydrides, based on aromatic and aliphatic dicarboxylic acids, which can be used as carriers for therapeutic substances [22]; analysis of the adhesive properties of salbutamol particles, used in aerosol or dry powder inhalers [23]; and the study of the effects of DNase I on polyamidoamine dendrimers complexed with DNA [24]. (The formation of these complexes protects DNA from DNase I, an effect that is of current and potential therapeutic significance in gene therapy, where it is necessary to protect DNA from degradation *in vivo*.)

Use of AFM to obtain structural information about membrane proteins

In drug development, interest is focused upon the interactions of drugs with receptors, most of which are proteins that either span or are intimately connected with the plasma membrane. The application of AFM to the investigation of membrane proteins has both limitations and advantages. First, membrane proteins are relatively difficult to isolate and purify, and even when they are successfully purified, it is necessary for them to be introduced into some form of lipid environment to produce conditions that might approximate to those prevailing in the cell. This latter factor has hampered the use of X-ray crystallography to elucidate the structure of membrane proteins. The difficulty arises because membrane proteins necessarily possess hydrophobic domains. It is possible to solubilize membrane proteins with detergents and thereby produce 3D crystals for X-ray crystallography, but this can lead to a reduction of the proteins' structural integrity. Consequently, the structures produced may not reflect the situation *in vivo*. By contrast, membrane proteins can be manipulated to produce 2D crystals in the presence of lipids, greatly increasing the likelihood that the behaviour of the protein will be physiologically relevant. In addition, the 2D crystal preparation upholds the native conformation of the proteins' hydrophilic loops, which are normally required for interaction with ligands and which are often compacted and immobilized in 3D crystals. Comprehensive details of procedures for 2D crystallization of membrane proteins are given in [13,25,26].

An example of the combination of 2D crystallization with AFM imaging to elucidate physiologically-relevant structural features of proteins is to be found in a series of papers by Engel and co-workers on members of the aquaporin family (AQPs, a superfamily of membrane water channels). In initial experiments [27], drawing on previous crystallographic work, the extracellular and cytoplasmic faces of the *E. coli* channel AQP Z were imaged. The cytoplasmic face was identified by initial tagging of the N-terminus with a decahistidine (His_{10}) sequence. It was then shown that the topology of the protein changed substantially upon proteolytic cleavage of the N-terminus. More recently, the forces that stabilize the structure of human AQP1 (hAQP1) were studied with force spectroscopy [28]. AFM was first used as an imaging tool to identify individual hAQP1 tetramers in 2D crystals. The AFM tip was then attached to the C-terminus of hAQP1 and various secondary structural elements (α-helices and loops) were 'pulled-out' from the membrane while the single-molecule force curve was being recorded. Force peaks, reflecting the unfolding of secondary structural elements, could be interpreted in light of existing atomic models of hAQP1. These results are significant because they represent a direct assessment of intermolecular forces delineating the oligomeric state of a membrane protein – and such oligomerization states are often crucial to our understanding of ligand-receptor interactions, as will be discussed in more detail below.

In a further study on the structure-function relationship of aquaporins, Fotiadis *et al.* [29] have shown that aquaporins possess domains that are highly likely to be involved in binding calcium. Comparison of images of hAQP1 and bovine AQP revealed significant structural differences, but also remarkable homogeneity in the regions encoded by an EF-hand motif. This region in turn showed significant homology with the EF-hand motifs of the calmodulin Ca^{2+}-binding protein superfamily. In further experiments, 2D crystals of AQP1 were treated with carboxypeptidase Y to cleave off the intracellular C-terminus, and difference maps of AFM images of native and the carboxypeptidase-treated AQPs were constructed (Figure 2). These maps indicated that the carboxyl tail is located close to the fourfold symmetry-axis of the tetramer that forms AQP1. This finding suggests that this site might be significant with respect to channel gating, and demonstrates the use of AFM to determine functional features of membrane proteins. In cholangiocytes and inner medullary collecting duct cells of the kidney, AQPs mediate the transcellular transport of water through the apical domain of the plasma membrane. The hormone secretin induces bile secretion (and requisite water transport) in cholangiocytes, and triggers the translocation of AQP1 from an intracellular

vesicular pool to the plasma membrane. Arginine vasopressin likewise triggers the insertion of AQP2 into the apical membrane of inner medullary collecting duct cells. The actions of both hormones occur concomitantly with a rise in cytoplasmic Ca^{2+} levels, suggesting that Ca^{2+} interactions with AQPs might affect both the water permeability of the channels and their trafficking between cellular compartments.

AFM imaging of protein-ligand complexes

The interactions of small ligands (such as potential new drugs) with protein targets are typically studied by radioligand binding. This approach provides quantitative information, such as the affinity of the binding interaction, which is crucial to the process of drug development. Radioligand binding, however, sheds no light on the structure of the ligand-protein complex, and cannot reveal any effects of ligand binding on protein structure. This additional information might prove to be significant, especially under circumstances where the structure of the protein is not known. An attempt has been made recently to assess the ability of AFM imaging to provide this information, using the biotin and streptavidin as a model ligand-receptor pair [30]. Streptavidin is a 60-kDa homotetramer that binds biotin with an extraordinarily high affinity (K_D ~10^{-14} M). The biotin-streptavidin complex has been crystallized, and its structure solved at high resolution [31,32]. Because the biotin molecule (molecular mass 244 Da) is too small to be visualized by AFM, it was tagged with a short (152-base-pair; 50-nm) DNA rod. When these biotinylated rods were incubated with purified streptavidin and the resulting complexes were bound to mica, a variety structures were visualized by AFM, including unoccupied streptavidin, and streptavidin bound by one to four DNA rods. When two rods were bound to one streptavidin molecule, the angle between the rods was either acute or obtuse, as expected from the positions of the biotin binding sites seen in the crystal structure [31,32]. Interestingly, the apparent size of the streptavidin molecule was increased upon biotinylation, revealing an effect of ligand binding on the structure of the protein target. It is clear from this study that AFM can reveal significant details of the structure of potential drug targets, such as the relative orientations of ligand binding sites. It should be possible to apply the same technique to other receptors, the vast majority of which have not yet been crystallized.

Considerations of the architecture of ionotropic receptors

Fast synaptic transmission involves the operation of members of a superfamily of ligand-gated ion channels, which includes nicotinic acetylcholine receptors, $GABA_A$ receptors and $5HT_3$ receptors [33]. All of these receptors are important drug targets, being involved in muscle relaxation during surgery (acetylcholine receptors), sedation and the treatment of anxiety and epilepsy ($GABA_A$ receptors), and therapies for emesis and irritable bowel syndrome ($5\text{-}HT_3$ receptors). Furthermore, all of the receptors have a common structure, with five subunits arranged around a pseudo-5-fold axis that delineates an ion-selective transmembrane pore [33]. Almost always, the receptors contain more than one type of subunit, which show considerable sequence homology with each other. Although the subunit stoichiometry of some of the receptors has been determined, the arrangement of the subunits within the receptor is usually unknown.

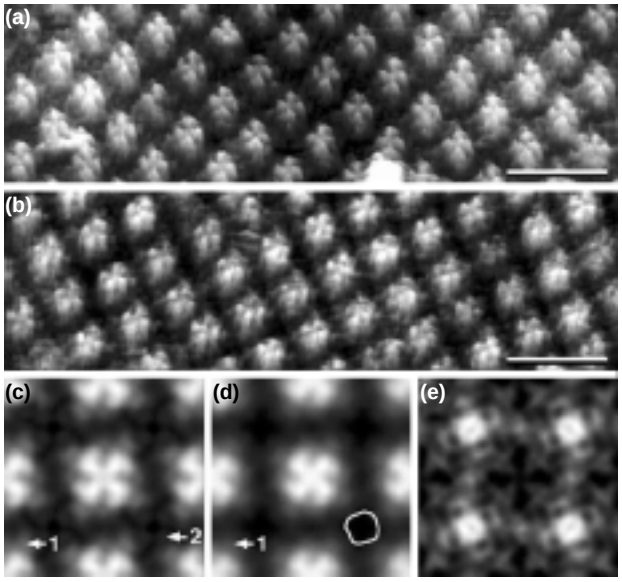

Figure 2. AFM imaging of human AQP1. **(a)** Surface topography of deglycosylated hAQP1 2D crystals before carboxypeptidase Y treatment. **(b)** Surface topography after carboxypeptidase Y treatment. **(c)** The symmetrized correlation average of the deglycosylated hAQP1 shows a windmill-like structure of 1.5 nm height on one side and a pronounced depression with windmill-shaped peripheral (1) and central protrusions (2) on the other side. **(d)** In the symmetrized correlation average of the deglycosylated and decarboxylated hAQP1, the high windmill-like structure was unchanged. On the lower side, the central protrusion (2) had disappeared while the peripheral one (1) appeared to be unaffected by the digestion. **(e)** Differences are evident in this difference map between the undigested and digested hAQP1 topographs [see contours in (d)]. Scale bars for (a) and (b) are 20 nm. The frame size of (c), (d) and (e) is 19.2 nm. Vertical brightness ranges (black equivalent to lowest feature, white to highest): (a) 2.2 nm, (b) 1.8 nm, (c) 1.5 nm, (d) 1.8 nm, and (e) 0.6 nm. The raw images in (a) and (b) are displayed as reliefs tilted by 28. This figure is reproduced, with permission, from Reference [29], where more details are given.

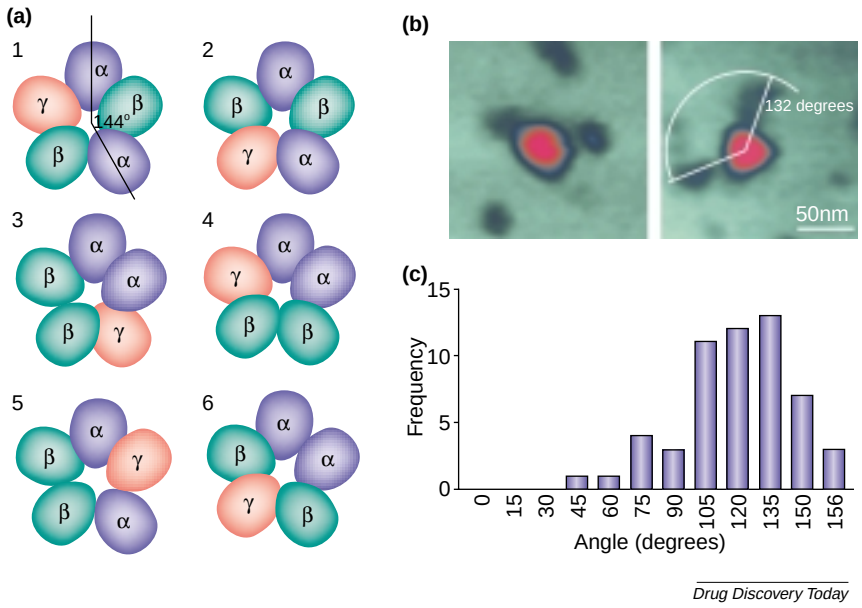

Figure 3. Analysis of $GABA_A$ receptor architecture by AFM. **(a)** Possible arrangements of subunits in a $GABA_A$ receptor composed of 2α-, 2β- and 1γ-subunits. Note that the angle between each subunit is 72°, assuming that the subunits are arrranged with five-fold pseudosymmetry. In arrangements 1, 2 and 5, there will be an angle of 144° between tags on the α-subunits. **(b)** AFM images of 1:2 complexes between $GABA_A$ receptors, with His_6 tags on their α-subunits, and mouse monoclonal anti-His_6 immunoglobulin G molecules. **(c)** Distribution of angles between antibody molecules in 1:2 complexes between $GABA_A$ receptors and anti-His_6 immunoglobulin G. Note the major peak at 135° and the possible minor peak at 75°.

The $GABA_A$ receptor, the major inhibitory neurotransmitter receptor in the brain, exists as a complex of five subunits, arranged around a central chloride ion channel [34]. Nineteen subunit isoforms have so far been identified [35]. It is thought that the predominant form of the receptor in the brain contains α_1-, β_2-, and γ_2-subunits [36], most likely in the stoichiometry 2α:2β:1γ [37]. The arrangement of the subunits around the receptor rosette, which has still not been established, is a significant issue because it is known that important drug binding sites are located at the interfaces between different subunits. Since GABA binding sites are between the α and β subunits [38], while benzodiazepine binding sites are between the α- and γ-subunits [39], it is unlikely that the two α-subunits are adjacent. In fact, previous work in which single-, double- and triple-subunit constructs were expressed in various combinations in *Xenopus* oocytes suggested an arrangement of γβαβα, reading counter-clockwise around the pore as viewed from the extracellular face [40,41].

An attempt has been made recently to develop an AFM-based methodology that can be used to determine the architecture of multi-subunit receptors in general and the $GABA_A$ receptor in particular [42]. There are six possible subunit arrangements in a $GABA_A$ receptor of stoichiometry 2α:2β:1γ (1–6 in Figure 3a). Assuming a five-fold pseudo-symmetry, the angle between each subunit will be 72°. Consequently, if the arrangement of the subunits is indeed γβαβα (arrangement 1), then the angle between the two α-subunits (and also between the two β-subunits) should be 144°. In a preliminary study, a hexahistidine (His_6) tag was engineered onto the C-terminus of the α-subunit and cells were transfected with DNA encoding α_1-, β_2-, and γ_2-subunits. The cells produced receptors containing all three subunits and delivered them to the plasma membrane. The His_6-tag was used to purify the receptor from membrane fractions of the transfected cells. The purified receptors were incubated with an anti-His_6 immunoglobulin G. The resulting receptor-immunoglobulin G complexes were bound to mica and imaged by AFM. Analysis of complexes containing two bound antibodies (Figure 3b) showed that the most common angle between the two antibody tags was 135° (Figure 3c), close to the value of 144° expected if the two α-subunits are separated by a third subunit. This result allows us to exclude three of the six possible arrangements of the subunits around the receptor rosette (3, 4 and 6 in Figure 3a). Intriguingly, the distribution of angles between the two bound antibodies hints at the presence of a small population with an angle of 75°, which suggests that the two α-subunits might be adjacent in a small proportion of the receptors. Hence, there might not be one fixed configuration of the receptor. As noted above, only a single-molecule imaging technique such as AFM can provide this type of information. This pilot study demonstrates that in principle this AFM-based approach will permit the complete elucidation of the structures of several therapeutically significant receptors.

Studies of interactions between drugs and DNA

The binding of ligands to DNA so as to alter its structure and function is important in various therapies for cancer, and in the aetiology of various infectious diseases, and gene targeting consequently offers hope for the treatment of a wide spectrum of diseases of genetic origin. As it

happens, DNA lends itself to investigation with AFM: lengths of DNA suitable for imaging can be produced in the laboratory, and the base sequence of the DNA can be designed so as to confer particular physical properties upon the molecule, or to generate targets for drug or protein binding. Early imaging experiments focused on the action of crosslinking compounds such as cisplatin and carbyplatin. In the late 1990s Onoa *et al.* [43] used AFM to investigate the mode of action on DNA of various platinum- and palladium-containing compounds. These studies were of interest because although it was clear that cisplatin, the 'classical' anti-cancer drug of its type, acts by targeting nitrogen atoms of DNA bases, no clear understanding existed concerning the effect of its interaction on the DNA structure. It was shown that cisplatin produced shortening in *hlyM* DNA (a 260 bp fragment from the haemolysin operon of *E.coli*), while other analogous compounds produced various effects, including aggregation and compaction, besides shortening. In later work Pang *et al.* [44] compared the effects of cisplatin and its inactive analogue transplatin on the morphology of polynucleotides. AFM revealed several enlarged ends of molecules in untreated poly-AT nucleotides, perhaps due to unwinding and/or collapse of regions of the DNA. On the other hand, poly-GC molecules showed no such features, except in the presence of cisplatin. Transplatin produced different features, causing overlapping or stacking of the polymer molecules. These results are interesting because cisplatin is known to target mainly the N_7 of guanine.

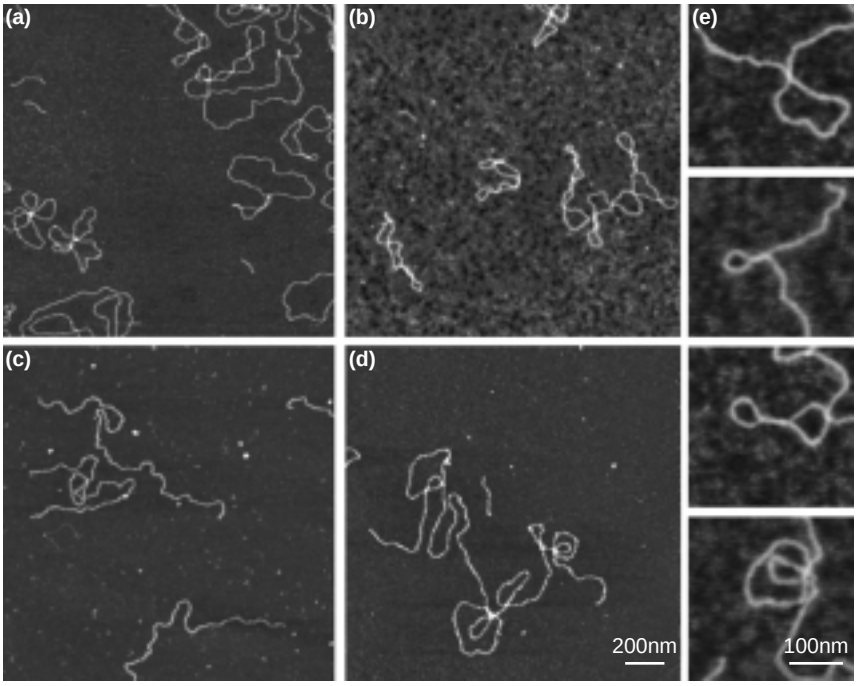

Figure 4. Bis-intercalation of ditercalinium into linear and circular plasmid DNA. Naked circular **(a)** and linear **(c)** forms of the 4.36-kb plasmid pBR322 were imaged by AFM, using tapping mode in air. The circular plasmids show some supercoiling, whereas the linear plasmids show a relaxed, extended conformation with few overlapping strands. After bis-intercalation of ditercalinium (at a molar drug:DNA ratio of 25:1), both circular **(b)** and linear **(d)** DNA molecules exhibited increased looping and close DNA-DNA contacts. **(e)** Shows loop structures found on linearized plasmids. The thick-stranded features are made by the tight coiling of two individual DNA strands. Height information for all images is colour-coded (dark [low]; light [high]). Scale bars: 200 nm (a–d), 100 nm (e). This figure is adapted, with permission, from Reference [49].

More sophisticated interactions between DNA and intercalating drugs have also been examined. The effects of the mono-intercalator ethidium bromide have been investigated using linear and circular plasmid DNA [45–47]. Changes in the tertiary structure of the DNA molecules were seen, and as the concentration of drug was increased, the DNA progressed from a relaxed structure, through a transitional phase of toroidal supercoiling, ultimately to structures with tight, plectonemic supercoils. Earlier experiments using electron microscopy previously showed that plectonemic supercoiling is the prevailing form adopted by plasmid DNA under the influence of ethidium bromide; hence, the toroidal form of supercoiling observed in the AFM study is unusual. This difference may reflect the advantages conferred by the more gentle preparation of DNA samples that is afforded by AFM, compared with electron microscopy. In further experiments, the same group applied force spectroscopy to an investigation of drug-DNA interactions [48]. They picked up single molecules of λ phage DNA with an AFM tip, and then investigated the extensibility of the DNA using force curves. They added in turn several drugs known to interact with DNA (berenil, which binds in the minor groove, cisplatin and ethidium bromide). Their results showed that extensibility was highly dependent upon the species of drug binding to the DNA, and that the dependence of extensibility on drug concentration was different for each agent. More complex effects on the properties of DNA are apparently produced by bisintercalating drugs. Berge *et al.* have recently performed mathematical analyses of the effects of two of these agents [49,50]. AFM of DNA in the presence

of the potent anti-tumour bisintercalating agent dercalinium demonstrates differences in the formation of supercoils and plectonemic coils (Figure 4; [49]), reflecting to some extent effects seen with monointercalators. Bisintercalators, however, function by a mechanism that is quite different from that of monointercalating drugs. Binding of the compound causes a structural deformation of the DNA helix that is recognized by repair systems, and it is the reversible nature of the deformation that causes malfunctioning of this DNA repair, eventually leading to cell death. Further analysis of the effects of drug binding performed with mixed-sequence DNA fragments, and using increment in contour length as a measure of intercalation, revealed saturation occurring at a point where sufficient drug was present to interact with every other available binding site. In addition, the apparent persistence length of the molecules was close to twice that of native DNA. In a further series of experiments, imaging and contour length analysis were used to investigate the action of another bisintercalator, luzopeptin B [50]. Bisintercalation appeared to be inversely related to the proportion of GC content in the DNA investigated. In addition to the length increase, a higher proportion of DNA molecules displaying complex morphology was observed as the concentration of luzopeptin was increased, and the various manifestations of this complex morphology would seem to arise from both inter- and intramolecular cross-linking of the DNA caused by binding of luzopeptin, features that were directly displayed by AFM imaging. In their conclusion to [48] the authors suggest that, perhaps for screening purposes, 'force spectroscopy... promises to become a helpful and sensitive tool for the investigation of DNA-drug binding modes on the single molecule level.' The same applies to other manifestations of AFM for drug interactions with DNA in particular and with macromolecules in general.

Conclusions

AFM permits the high-resolution imaging of biological macromolecules, measurement of forces within and between molecules, and the dissection of macromolecules. All of these features provide the potential, either alone or in combination with other molecular biological techniques, to produce data of potential value to the pharmaceutical industry. As its use in bioimaging continues to grow it is highly likely that AFM will begin to make a significant impact on drug development.

Acknowledgements

We are grateful to the Biotechnology and Biological Research Council for supporting our work.

References

1 Binnig, G. *et al.* (1986) Atomic force microscope. *Phys. Rev. Lett.* 56, 930–933
2 Baró, A.M. *et al.* (1985) Determination of surface topography of biological specimens at high resolution by scanning tunnelling microscopy. *Nature* 315, 253–254
3 Teague, E.C. *et al.* (1982) 3-Dimensional stylus profilometry. *Wear* 83, 1–12
4 Bezanilla, M. *et al.* (1994) Motion and enzymatic degradation of DNA in the atomic force microscope. *Biophys. J.* 67, 2454–2459
5 Allen, S. *et al.* (1996) In situ observation of streptavidin-biotin binding on an immunoassay well surface using an atomic force microscope. *FEBS Lett.* 390, 161–164
6 Fisher, T.E. *et al.* (1999) The study of protein mechanics with the atomic force microscope. *Trends Biochem. Sci.* 24, 379–384
7 Marszalek, P.E. *et al.* (1999) Mechanical unfolding intermediates in titin molecules. *Nature* 402, 100–103
8 Oberhauser, A.F. *et al.* (2001) Stepwise unfolding of titin under force-clamp atomic force microscopy. *Proc. Natl. Acad. Sci. U.S.A.* 98, 468–472
9 Li, H. *et al.* (2002) Reverse engineering of the giant muscle protein titin. *Nature* 418, 998–1002
10 Oberhauser, A.F. *et al.* (2002) The mechanical hierarchies of fibronectin observed with single-molecule AFM. *J. Mol. Biol.* 319, 433–447
11 Marszalek, P.E. *et al.* (2001) Fingerprinting polysaccharides with single-molecule atomic force microscopy. *Nat. Biotechnol.* 19, 258–262
12 Marszalek, P.E. *et al.* (2002) Chair-boat transitions in single polysaccharide molecules observed with force-ramp AFM. *Proc. Natl. Acad. Sci. U.S.A.* 99, 4278–4283
13 Fotiadis, D. *et al.* (2002) Imaging and manipulation of biological structures with the AFM. *Micron* 33, 385–397
14 Hoh, J.H. *et al.* (1993) Structure of the extracellular surface of the gap junction by atomic force microscopy. *Biophys. J.* 65, 149–163
15 Müller, D.J. *et al.* (2002) Conformational changes in surface structures of isolated connexin 26 gap junctions. *EMBO J.* 21, 3598–3607
16 Schabert, F.A. *et al.* (1995) Native *Escherichia coli* OmpF porin surfaces probed by atomic force microscopy. *Science* 268, 92–94
17 Fotiadis, D. *et al.* (2000) Surface tongue-and-groove contours on lens MIP facilitate cell-to-cell adherence. *J. Mol. Biol.* 300, 779–789
18 Kakoulides, E.P. *et al.* (1998) Azocrosslinked poly(acrylic acid) for colonic delivery and adhesion specificity: *in vitro* degradation and preliminary *ex vivo* bioadhesion studies. *J. Control. Release* 54, 95–109
19 Danesh, A. *et al.* (2000) The discrimination of drug polymorphic forms from single crystals using atomic force microscopy. *Pharm. Res.* 17, 887–890
20 Danesh, A. *et al.* (2001) An *in situ* dissolution study of aspirin crystal planes (100) and (001) by atomic force microscopy. *Pharm. Res.* 18, 299–303
21 Nakanishi, M. and Noguchi, A. (2001) Confocal and probe microscopy to study gene transfection mediated by cationic liposomes with a cationic cholesterol derivative. *Adv. Drug Deliv. Rev.* 52, 197–207
22 Shen, E. *et al.* (2001) Microphase separation in bioerodible copolymers for drug delivery. *Biomaterials* 22, 201–210
23 Eve, J.K. *et al.* (2002) A study of single drug particle adhesion interactions using atomic force microscopy. *Int. J. Pharm.* 238, 17–27
24 Abdelhady, H.G. *et al.* (2003) Direct real-time molecular scale visualisation of the degradation of condensed DNA complexes exposed to DNase I. *Nucleic Acids Res.* 31, 4001–4005
25 Hasler, L. *et al.* (1998) 2D crystallization of membrane proteins: rationales and examples. *J. Struct. Biol.* 121, 162–171
26 Werten, P.J. *et al.* (2002) Progress in the analysis of membrane protein structure and function. *FEBS Lett.* 529, 65–72
27 Scheuring, S. *et al.* (1999) High resolution AFM topographs of the *Escherichia coli* water channel aquaporin Z. *EMBO J.* 18, 4981–4987
28 Möller, C. *et al.* (2003) Determining molecular forces that stabilize human aquaporin-1. *J. Struct. Biol.* 142, 369–378

29 Fotiadis, D. *et al.* (2002) Identification and structure of a putative Ca^{2+}-binding domain at the C terminus of AQP1. *J. Mol. Biol.* 318, 1381–1394
30 Neish, C.S. *et al.* (2002) Direct visualization of ligand-protein interactions using atomic force microscopy. *Br. J. Pharmacol.* 135, 1943–1950
31 Weber, P.C. *et al.* (1989) Structural origins of high-affinity biotin binding to streptavidin. *Science* 243, 85–88
32 Hendrickson, W.A. *et al.* (1989) Crystal structure of core streptavidin determined from mutliwavelength anomalous diffraction of synchotron radiation. *Proc. Natl. Acad. Sci. U. S. A.* 86, 2190–2194
33 Karlin, A. (2002) Emerging structure of the nicotinic acetylcholine receptors. *Nat. Rev. Neurosci.* 3, 102–114
34 Nayeem, N. *et al.* (1994) Quaternary structure of the native $GABA_A$ receptor determined by electron microscopic image analysis. *J. Neurochem.* 62, 815–818
35 Sieghart, W. *et al.* (1999) Structure and subunit composition of $GABA_A$ receptors. *Neurochem. Int.* 34, 379–385
36 McKernan, R.M. and Whiting, P.J. (1996) Which $GABA_A$-receptor subtypes really occur in the brain? *Trends Neurosci.* 19, 139–143
37 Farrar, S.J. *et al.* (1999) Stoichiometry of a ligand-gated ion channel determined by fluorescence resonance energy transfer. *J. Biol. Chem.* 274, 10100–10104
38 Amin, J. and Weiss, D.S. (1993) $GABA_A$ receptor needs two homologous domains of the β-subunit for activation by GABA but not by pentobarbital. *Nature* 366, 565–569
39 Buhr, A. and Sigel, E. (1997) A point mutation in the γ_2-subunit of γ-aminobutryric $acid_A$ receptors results in altered benzodiazepine binding site specificity. *Proc. Natl. Acad. Sci. U. S. A.* 94, 8824–8829
40 Baumann, S. *et al.* (2001) Subunit arrangement of γ-aminobutyric acid type A receptor. *J. Biol. Chem.* 276, 36275–36280
41 Baumann, S. *et al.* (2002) Forced subunit assembly in $\alpha_1\beta_2\gamma_2$ $GABA_A$ receptors: insight into the absolute arrangement. *J. Biol. Chem.* 277, 46020–46025
42 Neish, C.S. *et al.* (2003) Atomic force microscopy of ionotropic receptors bearing subunit-specific tags provides a method for determining receptor architecture. *Nanotechnology* 14, 864–872
43 Onoa, G.B. *et al.* (1998) Study of the interaction of DNA with cisplatin and other Pd(II) and Pt(II) complexes by atomic force microscopy. *Nucleic Acids Res.* 26, 1473–1480
44 Pang, D. *et al.* (2000) Atomic force microscopy examination of conformations of polynucleotides in response to platinum isomers: Significance of GC content at broken ends. *Int. J. Cancer* 90, 68–72
45 Coury, J.E. *et al.* (1996) A novel assay for drug-DNA binding mode, affinity, and exclusion number: scanning force microscopy. *Proc. Natl. Acad. Sci. U. S. A.* 93, 12283–12286
46 Pope, L.H. *et al.* (1999) Intercalation-induced changes in DNA supercoiling observed in real-time by atomic force microscopy. *Anal. Chim. Acta* 400, 27–32
47 Pope, L.H. *et al.* (2000) Atomic force microscopy studies of intercalation-induced changes in plasmid DNA tertiary structure. *J. Microsc.* 199, 68–78
48 Krautbauer, R. *et al.* (2002) Discriminating small molecule DNA binding modes by single molecule force spectroscopy. *FEBS Lett.* 510, 154–158
49 Berge, T. *et al.* (2002) Structural perturbations in DNA caused by bis-intercalation of ditercalinium visualized by atomic force microscopy. *Nucleic Acids Res.* 30, 2980–2986
50 Berge, T. *et al.* (2003) The binding mode of the DNA bisintercalator luzopeptin investigated using atomic force microscopy. *J. Struct. Biol.* 142, 241–246